View metadata, citation and similar papers at core.ac.uk

brought to you by CORE

provided by Crossref

Hindawi Publishing Corporation
Journal of Electrical and Computer Engineering
Volume 2013, Article ID 189436, 10 pages
http://dx.doi.org/10.1155/2013/189436

Hindawi

Research Article

Novel Complete Probabilistic Models of Random Variation in High Frequency Performance of Nanoscale MOSFET

Rawid Banchuin

Department of Computer Engineering, Siam University, 38 Petchkasem Road, Bangkok 10160, Thailand

Correspondence should be addressed to Rawid Banchuin; rawid_b@yahoo.com

Received 27 September 2012; Revised 30 January 2013; Accepted 31 January 2013

Academic Editor: Jan Van der Spiegel

Copyright © 2013 Rawid Banchuin. This is an open access article distributed under the Creative Commons Attribution License, which permits unrestricted use, distribution, and reproduction in any medium, provided the original work is properly cited.

The novel probabilistic models of the random variations in nanoscale MOSFET's high frequency performance defined in terms of gate capacitance and transition frequency have been proposed. As the transition frequency variation has also been considered, the proposed models are considered as complete unlike the previous one which take only the gate capacitance variation into account. The proposed models have been found to be both analytic and physical level oriented as they are the precise mathematical expressions in terms of physical parameters. Since the up-to-date model of variation in MOSFET's characteristic induced by physical level fluctuation has been used, part of the proposed models for gate capacitance is more accurate and physical level oriented than its predecessor. The proposed models have been verified based on the 65 nm CMOS technology by using the Monte-Carlo SPICE simulations of benchmark circuits and Kolmogorov-Smirnov tests as highly accurate since they fit the Monte-Carlo-based analysis results with 99% confidence. Hence, these novel models have been found to be versatile for the statistical/variability aware analysis/design of nanoscale MOSFET-based analog/mixed signal circuits and systems.

1. Introduction

Nanoscale MOSFET has been adopted in many recently proposed analog/mixed signal circuits and systems such as high speed amplifier [1–3], millimeter wave components [4–6], and analog-to-digital converter [7–9]. Of course, the high frequency performances of these circuits and systems can be determined by those of their intrinsic MOSFET which can be defined by two major MOSFET's parameters, entitled gate capacitance, C_g, and transition frequency, f_T.

Obviously, imperfection in MOSFET's properties at the physical level, for example, random dopant fluctuation, line edge roughness, and so forth, causes the fluctuations in many of its characteristics such as threshold voltage, V_t, channel width, W, and channel length, L, which in turn yields the random variations in its circuit level parameters, for example, drain current, I_d, transconductance, g_m, and so forth. These variations are crucial in the statistical/variability aware design of MOSFET-based analog/mixed signal circuits and systems particularly at the nanometer regimes since their magnitudes become relatively large percentages. Hence, there are many previous researches on analytical modeling of such variations, for example, [10–13] and so forth, on which the nanoscale CMOS technology has been focused. However, they did not mention anything about variations in C_g and f_T even though they also exist and greatly affect the high frequency performances of the MOSFET-based circuits and systems. For these variations, results of studies as graphical plots and numerical measurements have been reported in previous articles, for example, [14–16] and so forth. In [17], the relationship between the variance of C_g and that of f_T has been derived. Unfortunately, formulation of each of these variations has not been mentioned. Later, the physical level oriented analytical model of random variation in C_g has been originally proposed in [18]. However, this model has been derived based on the classical model of physical level fluctuation-induced MOSFET's characteristic variation [19] which is being replaced by its more up-to-date successors such as that in [20]. Furthermore, the model in [18] is incomplete since the modeling on f_T which is as important as C_g has not been performed. To the knowledge of the author, such modeling on f_T has never been performed.

Hence, the novel probabilistic models of the random variations in nanoscale MOSFET's high frequency performances have been proposed in this paper. Beside the variation in C_g, that in f_T has also been focused on. So, these models are complete. Both random dopant fluctuation and process variation effects such as line edge roughness, which are the major causes of the random variations in the MOSFET's high frequency characteristics [16], have been taken into account. The nanoscale MOSFET equation [21] has been used as the mathematical basis similarly to [11, 12, 18]. As the precise mathematical expressions in terms of physical parameters, these models have been found to be both analytic and physical level oriented. Unlike [18], the state of the art physical level fluctuation-induced characteristic variation model of MOSFET [20] has been adopted instead of the classical one [19]. As a result, part of the models for variation in C_g is more accurate and physical level oriented than its predecessor [18]. These novel models have been verified based on the 65 nm CMOS process technology by using the Monte-Carlo SPICE simulations of the benchmark circuits and the Kolmogorov-Smirnov goodness of fit tests as very accurate since they fit the results obtained from Monte-Carlo SPICE simulations with 99% confidence. So, they have been found to be the versatile for the statistical/variability aware analysis/design of nanoscale MOSFET-based analog/mixed signal circuits and systems.

2. The Proposed Models

In this section, the proposed models will be presented. Before proceeding further, it is worthy to give some foundation on the nanoscale MOSFET's equation. It can be seen from [21] that I_d of the nanoscale MOSFET can be given with the gate oxide capacitance expressed in term of gate oxide permittivity ε_{ox} and thickness t_{ox} as

$$I_d = W\frac{\varepsilon_{ox}}{t_{ox}}\left(V_{gs} - V_t\right)v_{sat}, \quad (1)$$

where v_{sat} and V_{gs} denote the saturation velocity [20] and gate to source voltage. So, g_m of the nanoscale MOSFET is given by using (1) as follows:

$$g_m = W\frac{\varepsilon_{ox}}{t_{ox}}v_{sat}. \quad (2)$$

At this point, the derivation of the proposed models will be given by starting from finding the analytical expression of C_g and f_T. Similar to [18], C_g can be defined as [22]

$$C_g \triangleq \frac{dQ_g}{dV_{gs}}, \quad (3)$$

where Q_g denotes the gate charge [22] which can be determined as a function of I_d by using the approach adopted from [23] as

$$Q_g = -\frac{W^2 L\varepsilon_{ox}}{\alpha_d I_d V_t t_{ox}}\int_0^{V_{gs}-V_t}\left(V_{gs} - V_c - V_t\right)^2 dV_c - Q_{B,\max}, \quad (4)$$

where α_d and $Q_{B,\max}$ denote the coulomb scattering coefficient and the maximum bulk charge, respectively.

So, Q_g of the nanoscale MOSFET can be found by using (1) and (4) as

$$Q_g = -\frac{WL\left(V_{gs} - V_t\right)^2}{3\alpha_d v_{sat} V_t} - Q_{B,\max}. \quad (5)$$

As a result, C_g can be given by using (3) and (5) as follows:

$$C_g = \frac{2}{3}\frac{WL}{\alpha_d v_{sat}}\frac{V_t - V_{gs}}{V_t}. \quad (6)$$

At this point, the analytical expression of f_T can be immediately given by using (2) and (6) as follows:

$$f_T = \frac{3}{4}\frac{\alpha_d \varepsilon_{ox} v_{sat}^2}{t_{ox} L}\frac{V_t}{V_t - V_{gs}}. \quad (7)$$

By taking random dopant fluctuation and process variation effects into account, fluctuations in V_t, W, L, and so forth, denoted by ΔV_t, ΔW, ΔL, and so on, existed which yield random variations in C_g and f_T denoted by ΔC_g and Δf_T, respectively. This can be stated alternatively that ΔC_g and Δf_T are functions of ΔV_t, ΔW, ΔL, and so forth. With this in mind, ΔC_g and Δf_T can be mathematically defined as

$$\begin{aligned} \Delta C_g &\triangleq C_g\left(\Delta V_t, \Delta W, \Delta L, \ldots\right) - C_g, \\ \Delta f_T &\triangleq f_T\left(\Delta V_t, \Delta W, \Delta L, \ldots\right) - f_T, \end{aligned} \quad (8)$$

where $C_g\left(\Delta V_t, \Delta W, \Delta L, \ldots\right)$ and $f_T\left(\Delta V_t, \Delta W, \Delta L, \ldots\right)$ denoted the fluctuated C_g and f_T as functions of ΔV_t, ΔW, ΔL, and so on which are distributed in the Gaussian fashion. By using (6), (7), and (8), ΔC_g and Δf_T can be given in terms of physical level variables as follows:

$$\begin{aligned} \Delta C_g &= \frac{2}{3}\frac{(W+\Delta W)(L+\Delta L)}{\alpha_d v_{sat}}\frac{(V_t+\Delta V_t) - V_{gs}}{V_t + \Delta V_t} - \frac{2}{3}\frac{WL}{\alpha_d v_{sat}}\frac{V_t - V_{gs}}{V_t} \\ &\approx \frac{2WLV_{gs}\left(V_{FB} + 2\varphi_B - V_{tf}\right)}{3\alpha_d v_{sat}\left(V_{FB} + 2\varphi_B\right)^2}, \\ \Delta f_T &= \frac{3}{4}\frac{\alpha_d \varepsilon_{ox} v_{sat}^2}{(t_{ox}+\Delta t_{ox})(L+\Delta L)}\frac{V_t + \Delta V_t}{(V_t+\Delta V_t) - V_{gs}} - \frac{3}{4}\frac{\alpha_d \varepsilon_{ox} v_{sat}^2}{t_{ox} L}\frac{V_t}{V_t - V_{gs}} \\ &\approx \frac{3\alpha_d \varepsilon_{ox} v_{sat}^2 V_{gs}\left(V_{FB} + 2\varphi_B - V_{tf}\right)}{4\pi t_{ox} L\left(V_{gs} - V_{FB} - 2\varphi_B\right)^2}, \end{aligned} \quad (9)$$

where V_{FB}, V_{tf}, and φ_B denote flat band voltage, fluctuated threshold voltage, and half of surface band bending at inversion, respectively. Like other variations, Δt_{ox} denotes

random variation in t_{ox}. The summation of V_{FB} and φ_B approximates the threshold voltage which its fluctuation is the dominant one. It can be seen that the deterministic behaviors of ΔC_g and Δf_T can be analytically modeled by using (9).

For the probabilistic modeling of our interested the probability density functions of ΔC_g and Δf_T, denoted by $\mathrm{pdf}_{\Delta C_g}(\delta C_g)$ and $\mathrm{pdf}_{\Delta f_T}(\delta f_T)$, where δC_g and δf_T stand for any sampled value of ΔC_g and that of Δf_T, respectively, must be derived. In order to do so, the up-to-date model of physical level fluctuations-induced variation in MOSFET's characteristic [20] has been adopted. At this point, $\mathrm{pdf}_{\Delta C_g}(\delta C_g)$ and $\mathrm{pdf}_{\Delta f_T}(\delta f_T)$ can be, respectively, derived by using (9) and the basis model as in (10) and (11), where N_{eff} and W_d denote effective doping concentration and depletion region width, respectively [20].

Consider,

$$\mathrm{pdf}_{\Delta C_g}(\delta C_g) = \frac{4.33}{\sqrt{8\pi}} \frac{\alpha_d\, \varepsilon_{ox}\, v_{\mathrm{sat}} (V_{\mathrm{FB}} + 2\varphi_B)^2}{\sqrt{q t_{\mathrm{ox}} N_{\mathrm{eff}} W_d WL}\, V_{\mathrm{gs}}} \times \exp\left[-\frac{2.344 \alpha_d^2\, \varepsilon_{\mathrm{ox}}^2\, v_{\mathrm{sat}}^2 (V_{\mathrm{FB}} + 2\varphi_B)^4 \delta C_g^2}{q t_{\mathrm{ox}} N_{\mathrm{eff}} W_d WL V_{\mathrm{gs}}^2} \right], \tag{10}$$

$$\mathrm{pdf}_{\Delta f_T}(\delta f_T) = \frac{\sqrt{\pi} (V_{\mathrm{gs}} - V_{\mathrm{FB}} - 2\varphi_B)^2}{q \alpha_d\, v_{\mathrm{sat}}^2 V_{\mathrm{gs}}} \sqrt{\frac{t_{\mathrm{ox}} WL^3}{0.54 N_{\mathrm{eff}} W_d}} \times \exp\left[-\frac{1.852\pi^2 (V_{\mathrm{gs}} - V_{\mathrm{FB}} - 2\varphi_B)^4 t_{\mathrm{ox}} WL^3 \delta f_T^2}{q^2\, \alpha_d^2\, v_{\mathrm{sat}}^4 V_{\mathrm{gs}}^2\, N_{\mathrm{eff}} W_d} \right]. \tag{11}$$

Finally, the novel complete probabilistic models of the random variations in nanoscale MOSFET's high frequency performances have been now derived. By using these models and conventional statistical mathematics, the probabilistic/statistical behaviors of ΔC_g, Δf_T and even variations in other nanoscale MOSFET's high frequency parameters can be analytically explained in terms of related physical level variables. These models can be the mathematical tool for the statistical/variability aware optimization of MOSFET's high frequency performance and computer aid sensitivity analysis-based variability aware simulations of any circuit/system's high frequency parameters. The required computational effort has been found to be lower than that of the traditional Monte-Carlo analysis based on variation of MOSFET's characteristic which is time expensive [24]. Even though these models are oriented to variations in a single device, they can also be the modeling basis of mismatches in high frequency performances between transistors. These points will be discussed later.

Compared with [17] which proposed the relationship between the variance of C_g and that of f_T as [17]

$$(f_{T,\mathrm{mean}})^{-2} \sigma_{f_T}^2 = (g_{m,\mathrm{mean}})^{-2} \sigma_{g_m}^2 + (C_{g,\mathrm{mean}})^{-2} \sigma_{C_g}^2. \tag{12}$$

The models proposed in this paper, that is, $\mathrm{pdf}_{\Delta C_g}(\delta C_g)$ and $\mathrm{pdf}_{\Delta f_T}(\delta f_T)$ shown in (10) and (11), respectively, are more precise as they are the probability density functions in terms of physical level parameters such as W, L, and V_{FB}.

Furthermore, compared with the previous model in [18] composed of only one expression which models ΔC_g as [18]

$$\mathrm{pdf}_{\Delta C_g}(\delta C_g) = \frac{3\alpha_d v_{\mathrm{sat}} V_t}{2\sqrt{2\pi} A_{VT} \sqrt{WL}} \exp\left[\frac{9\alpha_d^2 v_{\mathrm{sat}}^2 V_t^2 \delta C_g^2}{8 A_{VT}^2 WL} \right]. \tag{13}$$

The models proposed in this research are more up-to-date and complete because they are derived based on newer basis model [20], and the previously overlooked Δf_T has now been modeled as $\mathrm{pdf}_{\Delta f_T}(\delta f_T)$ in (11). Moreover, $\mathrm{pdf}_{\Delta C_g}(\delta C_g)$ in (10) is more physical level oriented than its predecessor [18] as shown above since it contains additional physical level variables such as N_{eff}, W_d, and φ_B. The proposed $\mathrm{pdf}_{\Delta C_g}(\delta C_g)$ is more accurate than its predecessor as can be seen from its better goodness of fit test results shown in the upcoming section in which verification of both $\mathrm{pdf}_{\Delta C_g}(\delta C_g)$ and $\mathrm{pdf}_{\Delta f_T}(\delta f_T)$ will be given. Hence, these novel models have been found to be the potential mathematical tool for the variability aware analysis/design of various MOSFET-based analog/mixed signal circuits and systems at the nanometer regime.

3. The Verification

Verification of the proposed models has been performed in both qualitative and quantitative aspects. In the qualitative sense, $\mathrm{pdf}_{\Delta C_g}(\delta C_g)$ and $\mathrm{pdf}_{\Delta f_T}(\delta f_T)$ have been graphically compared with probability distributions of ΔC_g and Δf_T obtained from the Monte-Carlo SPICE simulations of the benchmark circuits affected by normally distributed fluctuations in characteristics of MOSFET such as V_t, W, and L. For verification in the quantitative manner, goodness of fit tests have been performed to $\mathrm{pdf}_{\Delta C_g}(\delta C_g)$ and $\mathrm{pdf}_{\Delta f_T}(\delta f_T)$. Since it has been suspected that ΔC_g and Δf_T are normally distributed via observation of the proposed models, the appropriate goodness of fit test has been found to KS test Here, overview of the KS test and its application to this research will be given. Strategy of the KS test is to performed the comparison of the K-S test statistic (KS) and the critical value (c) where it can be stated that any model fits its target data set if and only if its KS does not exceed its c [25, 26]. For this research, KS can be defined as

$$\mathrm{KS} = \max_{\delta x} \left\{ \left| \mathrm{CDF}'_{\Delta x}(\delta x) \right| - \left| \mathrm{CDF}_{\Delta x}(\delta x) \right| \right\}, \tag{14}$$

where Δx can be either ΔC_g or Δf_T so δx can be either δC_g or δf_T. As a result, $\mathrm{CDF}_{\Delta x}(\delta x)$ which represents the cumulative distribution function of any Δx can be either $\mathrm{CDF}_{\Delta C_g}(\delta C_g)$ for $\Delta x = \Delta C_g$ and $\delta x = \delta C_g$ or $\mathrm{CDF}_{\Delta f_T}(\delta f_T)$ for $\Delta x = \Delta f_T$ and $\delta x = \delta f_T$. Obviously, $\mathrm{CDF}_{\Delta C_g}(\delta C_g)$ can be obtained by using $\mathrm{pdf}_{\Delta C_g}(\delta C_g)$ as shown in (15) whereas $\mathrm{CDF}_{\Delta f_T}(\delta f_T)$ can be derived by using $\mathrm{pdf}_{\Delta f_T}(\delta f_T)$ as in (16).

Note that erf( ) denotes the error function which can be mathematically defined for arbitrary variable y as $\mathrm{erf}(y) = (2/\sqrt{\pi})\int_0^y \exp(-u^2)du$.

On the other hand, $\mathrm{CDF}'_{\Delta x}(\delta x)$ denotes the benchmark cumulative distribution function of any Δx which can be either ΔC_g or Δf_T, calculated by integration of its corresponding probability distribution obtained from simulations of benchmark circuits. Since the confidence level of the test is 99%, c can be given by (17), where n denotes the number of runs of Monte-Carlo SPICE analysis, which is chosen to be 3000 for this research. As a result, $c = 0.0297596$.

Consider,

$$\begin{aligned}\mathrm{CDF}_{\Delta C_g}(\delta C_g) &= \int_{-\infty}^{\delta C_g} \mathrm{pdf}_{\Delta C_g}(u)\,du \\ &= \frac{1}{2}\left\{1 + \mathrm{erf}\left[\frac{\sqrt{2.344}\alpha_d\,\varepsilon_{\mathrm{ox}} v_{\mathrm{sat}}(V_{\mathrm{FB}} + 2\varphi_B)^2 \delta C_g}{\sqrt{q t_{\mathrm{ox}} N_{\mathrm{eff}} W_d W L}\, V_{\mathrm{gs}}}\right]\right\},\end{aligned} \tag{15}$$

$$\begin{aligned}\mathrm{CDF}_{\Delta f_T}(\delta f_T) &= \int_{-\infty}^{\delta C_g} \mathrm{pdf}_{\Delta f_T}(v)\,dv \\ &= \frac{1}{2}\left\{1+\mathrm{erf}\left[\sqrt{\frac{1.852 t_{\mathrm{ox}} W L^3}{N_{\mathrm{eff}} W_d}}\,\frac{\pi(V_{\mathrm{gs}}-V_{\mathrm{FB}}-2\varphi_B)^2 \delta f_T}{q\,\alpha_d V_{\mathrm{gs}} v_{\mathrm{sat}}^2}\right]\right\},\end{aligned} \tag{16}$$

$$c = \frac{1.63}{\sqrt{n}}. \tag{17}$$

At this point, other issues such as verification basis, benchmark circuits, and simulation methodologies will be mentioned. As the nanoscale MOSFET is focused, the 65 nm CMOS process technology has been adopted as the verification basis. Similar to [18], parameterization of the proposed models has been performed by using the 65 nm CMOS process parameters, and the BSIM4-based benchmark circuits at 65 nm level with all necessary parameters extracted by Predictive Technology Model (PTM) [27] have been used. Of course, both NMOS and PMOS technologies have been considered.

In order to verify the accuracy of $\mathrm{pdf}_{\Delta C_g}(\delta C_g)$, the benchmark circuit and methodology used in [18] can be adopted. The core of this circuit for NMOS technological basis can be depicted in Figure 1, and C_g can be found as [18]

$$C_g = \frac{Y_{\mathrm{in}}}{j\omega} = \frac{1}{j\omega}\frac{I_{\mathrm{in}}}{V_{\mathrm{in}}}, \tag{18}$$

where Y_{in}, I_{in}, and V_{in} denote the input admittance, input current, and input voltage of the benchmark circuit, respectively. Similar to [18], the Monte-Carlo SPICE simulation of this circuit gives the benchmark probability distribution of ΔC_g

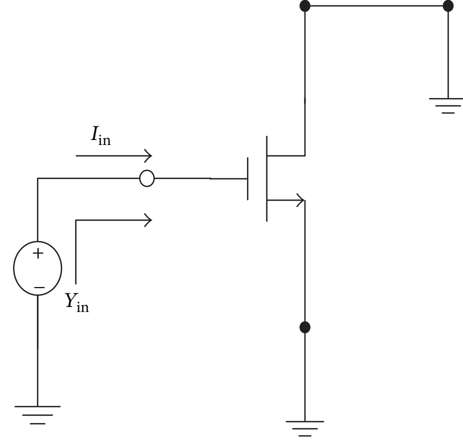

Figure 1: NMOS-based circuit for verifying $\mathrm{pdf}_{\Delta C_g}(\delta C_g)$ [18].

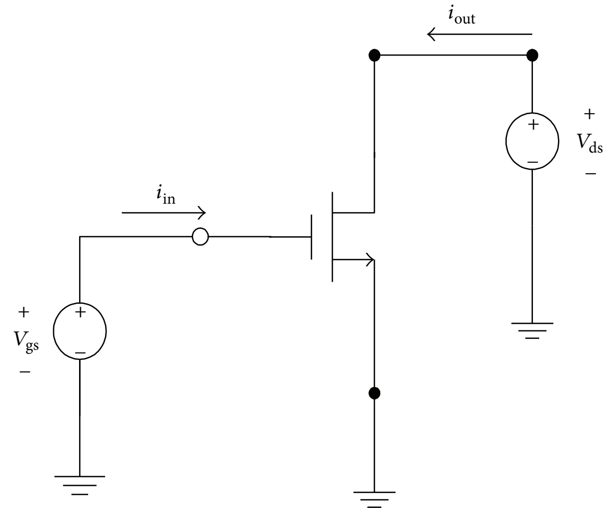

Figure 2: NMOS-based circuit for verifying $\mathrm{pdf}_{\Delta f_T}(\delta f_T)$.

for verification of $\mathrm{pdf}_{\Delta C_g}(\delta C_g)$ based on NMOS technology. For PMOS technology, the similar circuit with the NMOS device replaced with PMOS one and the similar methodology can be used as done in [18].

For verifying $\mathrm{pdf}_{\Delta f_T}(\delta f_T)$, core of the benchmark circuit can be depicted in Figure 2 for NMOS-based verification. From this circuit, f_T can be defined as the frequency in which the current gain is unity; that is, the magnitude of the small signal input current, $|i_{\mathrm{in}}|$ is equal to that of the output one, $|i_{\mathrm{out}}|$. Of course, the Monte-Carlo SPICE simulation of this circuit gives the benchmark probability distribution of Δf_T for verification of $\mathrm{pdf}_{\Delta f_T}(\delta f_T)$ based on NMOS technology. Of course, the similar circuit with the NMOS device replaced with PMOS one and the similar methodology can be used for PMOS technology-based verification. It should be mentioned here that all circuits operate under 1 V. supply voltage with $L = 60$ nm which is closed to the minimum allowable one, and $W = 1.2\,\mu$m. In the upcoming subsections, NMOS technology-based verification and PMOS-based one will be, respectively given; then it will be shown that $\mathrm{pdf}_{\Delta C_g}(\delta C_g)$ is more accurate than its predecessor.

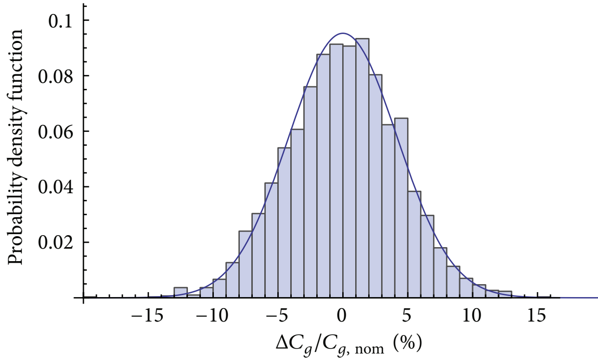

Figure 3: NMOS-based graphical comparison for the probability distribution of ΔC_g: $\text{pdf}_{\Delta C_g}(\delta C_g)$ (line) versus benchmark distribution from the circuit (histogram).

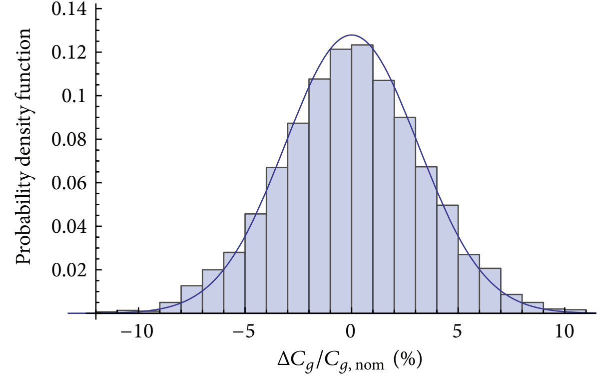

Figure 5: PMOS-based graphical comparison for the probability distribution of ΔC_g: $\text{pdf}_{\Delta C_g}(\delta C_g)$ (line) versus benchmark distribution from the circuit (histogram).

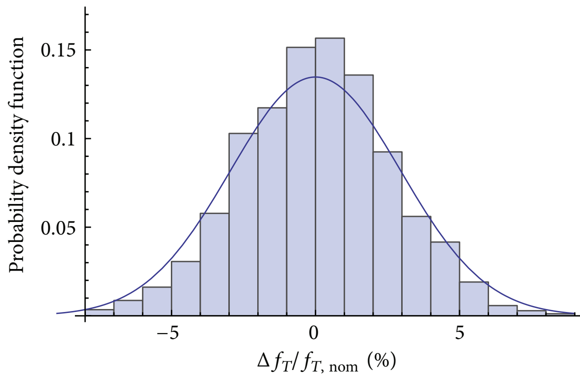

Figure 4: NMOS-based graphical comparison for the probability distribution of Δf_T: $\text{pdf}_{\Delta f_T}(\delta f_T)$ (line) versus benchmark distribution from the circuit (histogram).

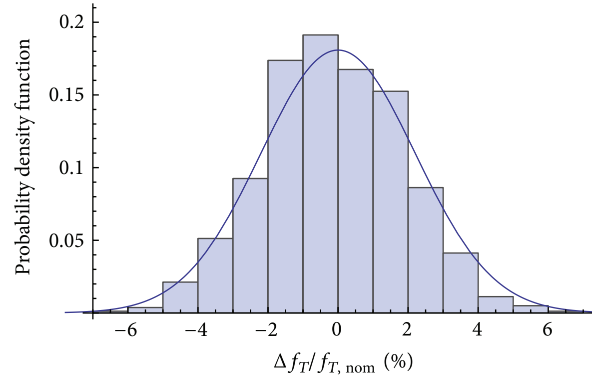

Figure 6: PMOS-based graphical comparison for the probability distribution of Δf_T: $\text{pdf}_{\Delta f_T}(\delta f_T)$ (line) versus benchmark distribution from the circuit (histogram).

3.1. NMOS-Based Verification. The graphical comparisons of the probability distributions are depicted in Figures 3 and 4 for verification in the qualitative sense of $\text{pdf}_{\Delta C_g}(\delta C_g)$ and that of $\text{pdf}_{\Delta f_T}(\delta f_T)$, respectively. The horizontal axes are labeled by $\Delta C_g/C_{g,\text{nom}}$ and $\Delta f_T/f_{T,\text{nom}}$ which display the amounts of ΔC_g and Δf_T as percentages of nominal $C_g, C_{g,\text{nom}}$ and nominal $f_T, f_{T,\text{nom}}$. A strong agreement between $\text{pdf}_{\Delta C_g}(\delta C_g)$ and its benchmark obtained from the Monte-Carlo simulation along with that between $\text{pdf}_{\Delta f_T}(\delta f_T)$ and its benchmark has been found. Furthermore, normal distributions of variations high frequency performances as predicted by the proposed models have been observed.

In the quantitative point of view, it can be seen that the resulting KS from the test of $\text{pdf}_{\Delta C_g}(\delta C_g)$ can be found as KS = 0.021463, and that from the test of $\text{pdf}_{\Delta f_T}(\delta f_T)$ is KS = 0.029223. These statistics do not exceed $c = 0.0297596$. This means that the proposed models can fit ΔC_g and Δf_T obtained from the Monte-Carlo SPICE simulation of NMOS-based circuits with 99% confidence. At this point, both $\text{pdf}_{\Delta C_g}(\delta C_g)$ and $\text{pdf}_{\Delta f_T}(\delta f_T)$ have been verified based on NMOS technology as highly accurate.

3.2. PMOS-Based Verification. The graphical comparisons of the probability distributions are depicted in Figures 5 and 6 for verification in the qualitative sense of $\text{pdf}_{\Delta C_g}(\delta C_g)$ and that of $\text{pdf}_{\Delta f_T}(\delta f_T)$. Strong agreements along with normal distributions of variations high frequency performances similar to those of NMOS-based verification have been found.

For verification in quantitative manner, on the other hand, KS from the test of $\text{pdf}_{\Delta C_g}(\delta C_g)$ can be found as KS = 0.016144 and that from the test of $\text{pdf}_{\Delta f_T}(\delta f_T)$ is KS = 0.029192. Similar to the previous NMOS-based case, these KS values do not exceed $c = 0.0297596$. This means that the proposed model can fit ΔC_g and Δf_T obtained from the simulation of PMOS-based circuits with 99% confidence. At this point, $\text{pdf}_{\Delta C_g}(\delta C_g)$ and $\text{pdf}_{\Delta f_T}(\delta f_T)$ are verified based on PMOS technology as highly accurate.

3.3. Higher Accuracy of $\text{pdf}_{\Delta C_g}(\delta C_g)$. In order to show that $\text{pdf}_{\Delta C_g}(\delta C_g)$ proposed in this research is more accurate than its predecessor, its KS statistics have been compared with those of such predecessor as given in [18]. Since the verification of the proposed $\text{pdf}_{\Delta C_g}(\delta C_g)$ and that of its

predecessor are identical, the comparison of the obtained statistics is said to be unbiased.

Obviously, the KS values obtained from verifying the proposed $\mathrm{pdf}_{\Delta C_g}(\delta C_g)$ which are 0.025466 for NMOS-based verification and 0.016144 for PMOS based are one, respectively-lower than those of the previous one in [18] given by 0.028462 for NMOS-based verification and 0.018036 for PMOS-based one [18]. According to [25, 26], this means $\mathrm{pdf}_{\Delta C_g}(\delta C_g)$ in this research is better fit to the simulated data than its predecessor [18] according to its lower KS statistics. This can be alternatively stated that the proposed $\mathrm{pdf}_{\Delta C_g}(\delta C_g)$ is more accurate.

4. Discussion

In this section, some discussions regarding to the applications of the proposed models introduced in the previous section and some verification results will be given.

4.1. Analytical Explanation of the Probabilistic/Statistical Behaviors of ΔC_g and Δf_T and Other Variations. The probabilistic/statistical behaviors of ΔC_g, Δf_T and variations in other high frequency parameters can be analytically explained by using their probabilistic/statistical parameters which can be derived by using the proposed $\mathrm{pdf}_{\Delta C_g}(\delta C_g)$ and $\mathrm{pdf}_{\Delta f_T}(\delta f_T)$ along with traditional statistical mathematic as analytical expressions involving physical level parameters. Simple examples of these parameters are means and variances of ΔC_g and Δf_T. They can be derived by applying statistical mathematic to $\mathrm{pdf}_{\Delta C_g}(\delta C_g)$ and $\mathrm{pdf}_{\Delta f_T}(\delta f_T)$ as follows:

$$\overline{\Delta C_g} = \int_{-\infty}^{\infty} \delta C_g \mathrm{pdf}_{\Delta C_g}\left(\delta C_g\right) d\delta C_g = 0, \tag{19a}$$

$$\begin{aligned} \sigma^2_{\Delta C_g} &= \int_{-\infty}^{\infty} \left(\delta C_g - \overline{\Delta C_g}\right)^2 \mathrm{pdf}_{\Delta C_g}\left(\delta C_g\right) d\delta C_g \\ &= \frac{q t_{\mathrm{ox}} N_{\mathrm{eff}} W_d WL V_{\mathrm{gs}}^2}{4.688\alpha_d^2 \varepsilon_{\mathrm{ox}}^2 v_{\mathrm{sat}}^2 (V_{\mathrm{FB}} + 2\varphi_B)^4}, \end{aligned} \tag{19b}$$

$$\overline{\Delta f_T} = \int_{-\infty}^{\infty} \delta f_T \mathrm{pdf}_{\Delta f_T}\left(\delta f_T\right) d\delta f_T = 0, \tag{20a}$$

$$\begin{aligned} \sigma^2_{\Delta f_T} &= \int_{-\infty}^{\infty} \left(\delta f_T - \overline{\Delta f_T}\right)^2 \mathrm{pdf}_{\Delta f_T}\left(\delta f_T\right) d\delta f_T \\ &= \frac{q^2 \alpha_d^2 v_{\mathrm{sat}}^4 V_{\mathrm{gs}}^2 N_{\mathrm{eff}} W_d}{3.704\pi^2 \left(V_{\mathrm{gs}} - V_{\mathrm{FB}} - 2\varphi_B\right)^4 t_{\mathrm{ox}} WL^3}, \end{aligned} \tag{20b}$$

where $\overline{\Delta C_g}$, $\sigma^2_{\Delta C_g}$, $\overline{\Delta f_T}$, and $\sigma^2_{\Delta f_T}$ denote mean and variance of ΔC_g along with those of Δf_T, respectively. Analytically obtaining these parameters yields various benefits to the statistical/variability aware analysis/design of nanoscale MOSFET-based analog/mixed signal circuits and systems, for example, obtaining the design tradeoffs which are important issues and so forth. A simple example of such design tradeoffs is shrinking the transistor dimension reduces ΔC_g with increasing of Δf_T as a penalty. This design tradeoff can be obtained from observations of (19b) and (20b) that $\sigma^2_{\Delta C_g} \propto WL$ and $\sigma^2_{\Delta f_T} \propto 1/WL^3$, respectively. It should be mentioned here that more sophisticated parameters such as moments of various orders, skewness, and kurtosis can also be derived by applying the statistical mathematic to $\mathrm{pdf}_{\Delta C_g}(\delta C_g)$ and $\mathrm{pdf}_{\Delta f_T}(\delta f_T)$.

An interesting joint parameter of ΔC_g and Δf_T is their correlation coefficient denoted by $\rho_{\Delta C_g,\Delta f_T}$, which defines their statistical relationship. $\rho_{\Delta C_g,\Delta f_T}$ can be given in terms of $\overline{\Delta C_g}$, $\sigma^2_{\Delta C_g}$, $\overline{\Delta f_T}$, and $\sigma^2_{\Delta f_T}$ as follows:

$$\rho_{\Delta C_g,\Delta f_T} = \frac{E\left[\left(\Delta C_g - \overline{\Delta C_g}\right)\left(\Delta f_T - \overline{\Delta f_T}\right)\right]}{\sqrt{\sigma^2_{\Delta C_g}}\sqrt{\sigma^2_{\Delta f_T}}}, \tag{21}$$

where $E[\ ]$ denotes the expectation operator. By using (9) and (19a)–(20b) which can be obtained from $\mathrm{pdf}_{\Delta C_g}(\delta C_g)$ and $\mathrm{pdf}_{\Delta f_T}(\delta f_T)$, along with (21), magnitude of $\rho_{\Delta C_g,\Delta f_T}$ has been found as unity. This means that there exists a very strong statistical relationship between ΔC_g and Δf_T.

As mentioned above, the analytical explanation of the probabilistic/statistical behaviors of variations in other high frequency parameters can be performed by using the $\mathrm{pdf}_{\Delta C_g}(\delta C_g)$ and $\mathrm{pdf}_{\Delta f_T}(\delta f_T)$ as these high frequency parameters are functions of C_g and/or f_T. Let any of such high frequency parameter and its variation be denoted by X and ΔX, respectively: ΔX can be given by

$$\Delta X = \left(\frac{\partial X}{\partial C_g}\right)\Delta C_g + \left(\frac{\partial X}{\partial f_T}\right)\Delta f_T. \tag{22}$$

Obviously, ΔX is a random variable where its probabilistic/statistical behavior can be analytically explained by using its probabilistic/statistical functions/parameters which can be derived by using either the proposed $\mathrm{pdf}_{\Delta C_g}(\delta C_g)$ and $\mathrm{pdf}_{\Delta f_T}(\delta f_T)$ or related parameters which are their functions such as $\overline{\Delta C_g}$, $\sigma^2_{\Delta C_g}$, $\overline{\Delta f_T}$, $\sigma^2_{\Delta f_T}$, and so forth. Simple examples of such functions/parameters of ΔX are its mean $\overline{\Delta X}$ and variance $\sigma^2_{\Delta X}$. They can be formulated in terms of $\overline{\Delta C_g}$, $\sigma^2_{\Delta C_g}$, $\overline{\Delta f_T}$, and $\sigma^2_{\Delta f_T}$ as follows:

$$\overline{\Delta X} = \left(\frac{\partial X}{\partial C_g}\right)\overline{\Delta C_g} + \left(\frac{\partial X}{\partial f_T}\right)\overline{\Delta f_T} = 0, \tag{23}$$

$$\begin{aligned} \sigma^2_{\Delta X} &= \left(\frac{\partial X}{\partial C_g}\right)^2 \sigma^2_{\Delta Cg} + \left(\frac{\partial X}{\partial f_T}\right)^2 \sigma^2_{\Delta fT} \\ &\quad + 2\left(\frac{\partial X}{\partial C_g}\right)\left(\frac{\partial X}{\partial f_T}\right)\sqrt{\sigma^2_{\Delta Cg}\sigma^2_{\Delta fT}}. \end{aligned} \tag{24}$$

Obviously, the fact that magnitude of $\rho_{\Delta C_g,\Delta f_T}$ is unity obtained by using $\mathrm{pdf}_{\Delta C_g}(\delta C_g)$ and $\mathrm{pdf}_{\Delta f_T}(\delta f_T)$ as stated

above has been used in the formulation of (24). By using (19a)–(20b) which can be obtained from the $\text{pdf}_{\Delta C_g}(\delta C_g)$ and $\text{pdf}_{\Delta f_T}(\delta f_T)$, (23) and (24), $\overline{\Delta X}$ and $\sigma^2_{\Delta X}$ can be derived as analytical expressions in terms of physical level parameters.

More sophisticatedly, the probability density function of ΔX denoted by $\text{pdf}_{\Delta X}(\delta X)$, where δX stands for the sample variable of ΔX, can be derived by using $\text{pdf}_{\Delta C_g}(\delta C_g)$ and $\text{pdf}_{\Delta f_T}(\delta f_T)$ along with a well-known statistical mathematic methodology entitled the transformation of random variables which can be found in the usual texts such as [28, 29], as ΔX is a function of ΔC_g and/or Δf_T, since X is a function of C_g and/or f_T as aforementioned. According to [28, 29], if ΔX is function of Δu which can be either ΔC_g or Δf_T as X is function of u which can be either C_g or f_T, $\text{pdf}_{\Delta X}(\delta X)$ can be given in a straightforward manner as

$$\text{pdf}_{\Delta X}(\delta X) = \text{pdf}_{\Delta u}(\delta u(\delta X)) \left[\left[\left| \frac{\partial \delta u}{\partial \delta X} \right| \right] \bigg|_{\delta u \to \delta u(\delta X)} \right]^{-1}, \tag{25}$$

where $\text{pdf}_{\Delta u}(\delta u(\delta X))$ stands for the probability density function of Δu denoted by $\text{pdf}_{\Delta u}(\delta u)$ with δu expressed in terms of δX. Since Δu can be either ΔC_g or Δf_T, $\text{pdf}_{\Delta u}(\delta u)$ can be either $\text{pdf}_{\Delta C_g}(\delta C_g)$ or $\text{pdf}_{\Delta f_T}(\delta f_T)$.

According to [29], if ΔX depends on both ΔC_g and Δf_T as X is a function of both C_g and f_T, $\text{pdf}_{\Delta X}(\delta X)$ can be given by

$$\text{pdf}_{\Delta X}(\delta X) = \int_{-\infty}^{\infty} l(\delta X, \delta Y)\, d\delta Y, \tag{26a}$$

where

$$l(\delta X, \delta Y) = \text{pdf}_{\Delta C_g, \Delta f_T}\left(\delta C_g(\delta X, \delta Y), \delta f_T(\delta X, \delta Y)\right) \times J(\delta X, \delta Y), \tag{26b}$$

$$J(\delta X, \delta Y) = \begin{vmatrix} \dfrac{\partial[\delta C_g(\delta X, \delta Y)]}{\partial \delta X} & \dfrac{\partial[\delta C_g(\delta X, \delta Y)]}{\partial \delta Y} \\ \dfrac{\partial[\delta f_T(\delta X, \delta Y)]}{\partial \delta X} & \dfrac{\partial[\delta f_T(\delta X, \delta Y)]}{\partial \delta Y} \end{vmatrix}, \tag{26c}$$

$$\delta C_g(\delta X, \delta Y) = \begin{vmatrix} \delta X & \dfrac{\partial X}{\partial f_T} \\ \delta Y & \dfrac{\partial Y}{\partial f_T} \end{vmatrix} \left[\begin{vmatrix} \dfrac{\partial X}{\partial C_g} & \dfrac{\partial X}{\partial f_T} \\ \dfrac{\partial Y}{\partial C_g} & \dfrac{\partial Y}{\partial f_T} \end{vmatrix} \right]^{-1}, \tag{26d}$$

$$\delta f_T(\delta X, \delta Y) = \begin{vmatrix} \dfrac{\partial X}{\partial C_g} & \delta X \\ \dfrac{\partial Y}{\partial C_g} & \delta Y \end{vmatrix} \left[\begin{vmatrix} \dfrac{\partial X}{\partial C_g} & \dfrac{\partial X}{\partial f_T} \\ \dfrac{\partial Y}{\partial C_g} & \dfrac{\partial Y}{\partial f_T} \end{vmatrix} \right]^{-1}, \tag{26e}$$

where δY denotes the sample variable of ΔY which stands for the variation in a conveniently chosen auxiliary function denoted by Y. Similar to X, Y is also a function of both C_g and f_T. It should be mentioned here that $\text{pdf}_{\Delta C_g, \Delta f_T}(\delta C_g(\delta X, \delta Y), \delta f_T(\delta X, \delta Y))$ can be found by applying (26d) and (26e) to $\text{pdf}_{\Delta C_g, \Delta f_T}(\delta C_g, \delta f_T)$ which stands for the joint probability density function of ΔC_g and Δf_T. This function can be found from the $\text{pdf}_{\Delta C_g}(\delta C_g)$ and $\text{pdf}_{\Delta f_T}(\delta f_T)$ by simultaneously solving the following equations:

$$\text{pdf}_{\Delta C_g}(\delta C_g) = \int_{-\infty}^{\infty} \text{pdf}_{\Delta C_g, \Delta f_T}(\delta C_g, \delta f_T)\, d\delta f_T, \tag{27a}$$

$$\text{pdf}_{\Delta f_T}(\delta f_T) = \int_{-\infty}^{\infty} \text{pdf}_{\Delta C_g, \Delta f_T}(\delta C_g, \delta f_T)\, d\delta C_g. \tag{27b}$$

The next subsection will discuss the application of $\text{pdf}_{\Delta C_g}(\delta C_g)$ and $\text{pdf}_{\Delta f_T}(\delta f_T)$ as the mathematical tool of the statistical/variability aware optimization scheme for nanoscale MOSFET's high frequency performance.

4.2. Mathematical Tool of Statistical/Variability Aware Optimization Scheme. Obviously, target of the optimization has been found to be minimizing ΔC_g and Δf_T. Simple objective functions can be obtained by using $\sigma^2_{\Delta C_g}$ and $\sigma^2_{\Delta f_T}$ which can be derived by using $\text{pdf}_{\Delta C_g}(\delta C_g)$ and $\text{pdf}_{\Delta f_T}(\delta f_T)$ as follows:

$$\begin{aligned} &\text{minimize}\left[\sigma^2_{\Delta C_g}\right], \\ &\text{minimize}\left[\sigma^2_{\Delta f_T}\right]. \end{aligned} \tag{28}$$

More sophisticatedly, the objective functions can be given in terms of $\Pr\{\Delta C_g = 0\}$ and $\Pr\{\Delta f_T = 0\}$ which stand for the probability of obtaining $\Delta C_g = 0$ and that of obtaining $\Delta f_T = 0$, respectively. These probabilities can be determined from $\text{pdf}_{\Delta C_g}(\delta C_g)$ and $\text{pdf}_{\Delta f_T}(\delta f_T)$ by using the mathematical foundation in [28] as follows:

$$\begin{aligned} \Pr\{\Delta C_g = 0\} &= \lim_{\chi \to 0}\left[\int_{-\chi}^{0} \text{pdf}_{\Delta C_g}(\delta C_g)\, d\delta C_g\right], \\ \Pr\{\Delta f_T = 0\} &= \lim_{\varphi \to 0}\left[\int_{-\varphi}^{0} \text{pdf}_{\Delta f_T}(\delta f_T)\, d\delta f_T\right], \end{aligned} \tag{29}$$

where $\chi \neq 0$ and $\varphi \neq 0$; moreover, they may or may not be equal to each other. In this case, the optimal MOSFET's parameters can be found by searching for those which maximize both $\Pr\{\Delta C_g = 0\}$ and $\Pr\{\Delta f_T = 0\}$. As a result, the objective functions can be now given by

$$\begin{aligned} &\text{maximize}\left[\Pr\{\Delta C_g = 0\}\right], \\ &\text{maximize}\left[\Pr\{\Delta f_T = 0\}\right]. \end{aligned} \tag{30}$$

If a single objective function optimization scheme is required, $\Pr\{\Delta C_g = 0, \Delta f_T = 0\}$ which is the probability to obtain $\Delta C_g = 0$ and $\Delta f_T = 0$ simultaneously, can be used. This probability can be defined as in (31), where $\text{pdf}_{\Delta C_g, \Delta f_T}(\delta C_g, \delta f_T)$ can be determined from $\text{pdf}_{\Delta C_g}(\delta C_g)$ and $\text{pdf}_{\Delta f_T}(\delta f_T)$ as shown in (27a) and (27b). In this case,

the optimal MOSFET's parameters can be found by searching for those which maximize $\Pr\{\Delta C_g = 0, \Delta f_T = 0\}$. As a result, the objective function can be obtained as in (32).

Consider,

$$\Pr\left\{\Delta C_g = 0, \Delta f_T = 0\right\} = \lim_{\varphi \to 0}\left[\lim_{\chi \to 0}\left[\left[\int_{-\varphi}^{0}\int_{-\chi}^{0} \mathrm{pdf}_{\Delta C_g,\Delta f_T}\left(\delta C_g, \delta f_T\right) d\delta C_g\, d\delta f_T\right]\right]\right], \tag{31}$$

$$\text{maximize } \left[\Pr\left\{\Delta C_g = 0, \Delta f_T = 0\right\}\right]. \tag{32}$$

The next subsection will give a discussion on the application of $\mathrm{pdf}_{\Delta C_g}(\delta C_g)$ and $\mathrm{pdf}_{\Delta f_T}(\delta f_T)$ as the mathematical tool of the variability aware simulation of nanoscale MOSFET's high frequency performance with reduced computational effort.

4.3. Mathematical Tool for Reduced Computational Effort Variability Aware Simulation of High Frequency Parameters. Obviously, outcome of any variability aware simulation is often expressed as the standard deviation of the simulated parameter. Let any interested high frequency parameter of variability aware simulation be Z, the desired outcome in terms of σ_Z can be conventionally determined by using the Monte-Carlo simulation which requires numerous runs [24]. So, many of the computational efforts are consumed.

On the other hand, σ_Z can be computed in a more computationally efficient manner by using the sensitivity of Z with respect to C_g and that with respect to f_T. These sensitivities can be determined by using the sensitivity analysis for which the targeted circuit/system is needed to be solved only once [24, 30]; then σ_Z can be simply computed by using $\sigma^2_{\Delta C_g}$ and $\sigma^2_{\Delta f_T}$ of MOSFETs within the targeted circuit/system. It can be seen that much of the computational effort for determining σ_Z is significantly reduced by using such sensitivity analysis-based method.

At this point, the sensitivity analysis-based computation of σ_Z will be explained. Let any circuits/systems compose M MOSFETs; σ_Z can be given in terms of $\sigma^2_{\Delta C_g}$ of any ith MOSFET, $\sigma^2_{\Delta C_g,i}$, that of any jth MOSFET, $\sigma^2_{\Delta C_g,j}$, $\sigma^2_{\Delta f_T}$ of any ith MOSFET $\sigma^2_{\Delta f_T,i}$, and that of any jth MOSFET, $\sigma^2_{\Delta f_T,j}$, as

$$\begin{aligned}\sigma_Z = \Bigg[&\sum_{i=1}^{M}\left[\left(S^Z_{C_g}\Big|_i\right)^2\sigma^2_{\Delta C_g,i} + \left(S^Z_{f_T}\Big|_i\right)^2\sigma^2_{\Delta f_T,i}\right] \\ &+ \sum_{\substack{i=1\\ i\neq j}}^{M}\sum_{j=1}^{M}\left[\left(S^Z_{C_g}\Big|_i\right)\left(S^Z_{C_g}\Big|_j\right)\rho_{\Delta C_g,i,\Delta C_g,j}\sqrt{\sigma^2_{\Delta C_g,i}}\sqrt{\sigma^2_{\Delta C_g,j}}\right. \\ &\left.+\left(S^Z_{f_T}\Big|_i\right)\left(S^Z_{f_T}\Big|_j\right)\rho_{\Delta f_T,i,\Delta f_T,j}\sqrt{\sigma^2_{\Delta f_T,i}}\sqrt{\sigma^2_{\Delta f_T,j}}\right] \\ &+ 2\sum_{i=1}^{M}\sum_{j=1}^{M}\left[\left(S^Z_{C_g}\Big|_i\right)\left(S^Z_{f_T}\Big|_j\right)\right. \\ &\left.\times \rho_{\Delta C_g,i,\Delta f_T,j}\sqrt{\sigma^2_{\Delta C_g,i}}\sqrt{\sigma^2_{\Delta f_T,j}}\right]\Bigg]^{1/2},\end{aligned} \tag{33}$$

where $\rho_{\Delta C_g,i;\Delta C_g,j}$, $\rho_{\Delta f_T,i;\Delta f_T,j}$ and $\rho_{\Delta C_g,i;\Delta f_T,j}$ denote correlation coefficient between ΔC_g of ith and jth MOSFET, that between Δf_T of ith and jth MOSFET, and that between ΔC_g of ith MOSFET and Δf_T of jth MOSFET, respectively. Their magnitudes can be approximated by unity when $i = j$. Furthermore, $S^Z_{C_g}|_i$, $S^Z_{C_g}|_j$, $S^Z_{f_T}|_i$, and $S^Z_{f_T}|_j$ denote sensitivity of Z to C_g of ith MOSFET, that to C_g of jth MOSFET, that to f_T of ith MOSFET, and that to f_T of jth MOSFET, respectively. These sensitivities can be determined by using the aforementioned sensitivity analysis. Finally, according to their definitions, $\sigma^2_{\Delta C_g,i}$ ($\sigma^2_{\Delta C_g,j}$) and $\sigma^2_{\Delta f_T,i}$ ($\sigma^2_{\Delta f_T,j}$) can be simply determined by substitution of the ith (jth) MOSFET's parameters into (19b) and (20b) which have been derived by using the proposed $\mathrm{pdf}_{\Delta C_g}(\delta C_g)$ and $\mathrm{pdf}_{\Delta f_T}(\delta f_T)$.

In the next subsection, the application of $\mathrm{pdf}_{\Delta C_g}(\delta C_g)$ and $\mathrm{pdf}_{\Delta f_T}(\delta f_T)$ as the mathematical basis for analytical modeling of the high frequency performances mismatches between theoretically identical nanoscale MOSFETs will be discussed.

4.4. Basis for Analytical Modeling of High Frequency Performances Mismatches. For illustration, the mismatch in C_g and that in f_T will be considered by letting such mismatches between theoretically identical devices, denoted by $\delta C_{gij} = C_{gi} - C_{gj}$ and $\delta f_{Tij} = f_{Ti} - f_{Tj}$ for mismatch in C_g and that in f_T, respectively. It should be mentioned here that C_{gi}, C_{gj}, f_{Ti}, and f_{Tj} denote C_g of ith MOSFET, C_g of jth MOSFET, f_T of ith MOSFET, and f_T of jth MOSFET.

Since the behaviors of mismatches can be conveniently modeled by their variances [31, 32], the modeling of δC_{gij} and δf_{Tij} is to derive their variances, that is, $\sigma^2_{\delta C_g ij}$ and $\sigma^2_{\delta f_T ij}$. Obviously the variances of C_{gi}, C_{gj}, f_{Ti}, and f_{Tj} which are fluctuated by the effects of random dopant fluctuation and process variation can be given by $\sigma^2_{\Delta C_g,i}$, $\sigma^2_{\Delta C_g,j}$, $\sigma^2_{\Delta f_T,i}$, and $\sigma^2_{\Delta f_T,j}$ due to (8). Of course, $\sigma^2_{\Delta C_g,i}$, $\sigma^2_{\Delta C_g,j}$, $\sigma^2_{\Delta f_T,i}$ and $\sigma^2_{\Delta f_T,j}$ can be determined by using $\mathrm{pdf}_{\Delta C_g}(\delta C_g)$ and $\mathrm{pdf}_{\Delta f_T}(\delta f_T)$ which are single devices oriented. In terms of these variances, $\sigma^2_{\delta C_g ij}$ and $\sigma^2_{\delta f_T ij}$ can be given as follows:

$$\begin{aligned}\sigma^2_{\delta C_g ij} &= \sigma^2_{\Delta C_g,i} + \sigma^2_{\Delta C_g,j} - 2\rho_{\Delta C_g i,\Delta C_g j}\sigma_{\Delta C_g,i}\sigma_{\Delta C_g,j}, \\ \sigma^2_{\delta f_T ij} &= \sigma^2_{\Delta f_T,i} + \sigma^2_{\Delta f_T,j} - 2\rho_{\Delta f_T i,\Delta f_T j}\sigma_{\Delta f_T,i}\sigma_{\Delta f_T,j}.\end{aligned} \tag{34}$$

Obviously, transistors are highly correlated if they are closely spaced [31, 32]. So, $\sigma^2_{\delta C_g ij}$ and $\sigma^2_{\delta f_T ij}$ are minimized if the correlations are in the positive manner and maximized if devices are negatively correlated. On the other hand,

Table 1: Max($\Delta C_g/C_{g,\mathrm{nom}}$) and Max($\Delta f_T/f_{T,\mathrm{nom}}$).

Max($\Delta C_g/C_{g,\mathrm{nom}}$) (%)		Max($\Delta f_T/f_{T,\mathrm{nom}}$) (%)	
NMOS	PMOS	NMOS	PMOS
14.037	10.6	7.676	6.023

Table 2: K-S test statistics.

From verification of $\mathrm{pdf}_{\Delta C_g}(\delta C_g)$		From Δf_T verification of $\mathrm{pdf}_{\Delta f_T}(\delta f_T)$	
NMOS	PMOS	NMOS	PMOS
0.021463	0.016144	0.029223	0.029192

correlation terms can be neglected from (34) if devices are distanced [31, 32]. In the final subsection, discussion regarding observations from the verification results will be given.

4.5. Observations from Verification Results. It can be observed from the formerly shown Monte-Carlo SPICE simulation results that the maximum percentages of ΔC_g and Δf_T denoted by Max[$\Delta C_g/C_{g,\mathrm{nom}}$] and Max[$\Delta f_T/f_{T,\mathrm{nom}}$], respectively, obtained from the NMOS-based circuits are higher than their counterparts from the PMOS ones. These maximum percentages are listed in Table 1. This means that high frequency performances of the nanoscale PMOS transistor is more robust to the random dopant fluctuation and process variation effects than that of NMOS one due to its lower Max[$\Delta C_g/C_{g,\mathrm{nom}}$] and Max[$\Delta f_T/f_{T,\mathrm{nom}}$].

Furthermore, it has been observed that the KS values obtained from the PMOS-based verification are smaller than those obtained from the NMOS-based one. These statistics are repeated in Table 2 for convenience. This means that the proposed $\mathrm{pdf}_{\Delta C_g}(\delta C_g)$ and $\mathrm{pdf}_{\Delta f_T}(\delta f_T)$ model ΔC_g and Δf_T of nanoscale PMOS transistor more accurately than they do to ΔC_g and Δf_T of NMOS device according to such smaller statistics.

5. Conclusion

The novel complete probabilistic models of the random variations in nanoscale MOSFET's high frequency performances have been proposed in this research as $\mathrm{pdf}_{\Delta C_g}(\delta C_g)$ and $\mathrm{pdf}_{\Delta f_T}(\delta f_T)$, shown in (10) and (11) as respectively. They have been found to be both analytic and physical level oriented as many physical level variables have been involved. Obviously, the formerly overlooked Δf_T has been now focused on. Both random dopant fluctuation and process variation effects have been taken into account. The nanoscale MOSFET equation [21] has been used as the mathematical basis, and the state of the art physical level fluctuation-induced characteristic variation model of MOSFET [20] has been adopted. So, $\mathrm{pdf}_{\Delta C_g}(\delta C_g)$ is more accurate and physical level oriented than its predecessor [18]. Both $\mathrm{pdf}_{\Delta C_g}(\delta C_g)$ and $\mathrm{pdf}_{\Delta f_T}(\delta f_T)$ have been verified based on the 65 nm CMOS process technology by using the Monte-Carlo SPICE simulations of the benchmark circuits and the Kolmogorov-Smirnov goodness of fit tests as very accurate since they fit the results of Monte-Carlo SPICE simulations with 99% confidence. Furthermore, they have various utilities such as analytical explanation of probabilistic/statistical behaviors of such random variations and others, as mentioned above. So, they have been found to be versatile for the statistical/variability aware analysis/design of nanoscale MOSFET-based analog/mixed signal circuits and systems.

Acknowledgment

The author would like to acknowledge Mahidol University, Thailand, for online database service.

References

[1] T. Yao, M. Gordon, K. Yau, M. T. Yang, and S. P. Voinigescu, "60-GHz PA and LNA in 90-nm RF-CMOS," in *Proceedings of the IEEE Radio Frequency Integrated Circuits Symposium*, pp. 147–150, San Francisco, Calif, USA, June 2006.

[2] M. A. Masud, H. Zirath, M. Ferndahl, and H. O. Vickes, "90 nm CMOS MMIC amplifier," in *Proceedings of the IEEE Radio Frequency Integrated Circuits (RFIC) Symposium*, pp. 201–204, Forth Worth, Tex, USA, June 2004.

[3] Y. S. Jiang, Z. M. Tsai, J. H. Tsai, H. T. Chen, and H. Wang, "A 86 to 108 GHz amplifier in 90 nm CMOS," *IEEE Microwave and Wireless Components Letters*, vol. 18, no. 2, pp. 124–126, 2008.

[4] B. Heydari, M. Bohsali, E. Adabi, and A. M. Niknejad, "Low-power mm-wave components up to 104 GHz in 90 nm CMOS," in *Proceedings of the 54th IEEE International Solid-State Circuits Conference (ISSCC'07)*, pp. 200–597, San Francisco, Calif, USA, February 2007.

[5] M. Varonen, M. Kärkkäinen, M. Kantanen, and K. A. I. Halonen, "MM-wave integrated circuits in 65-nm CMOS," *IEEE Journal of Solid-State Circuits*, vol. 43, no. 9, pp. 1991–2002, 2008.

[6] A. M. Niknejad, S. Emami, B. Heydari, M. Bohsali, and E. Adabi, "Nanoscale CMOS for mm-wave applications," in *Proceedings of the IEEE Compound Semiconductor Integrated Circuit Symposium (CSIC'07)*, pp. 1–4, Portland, Ore, USA, October 2007.

[7] D. Draxelmayr, "A 6 b 600 MHz 10 mW ADC array in digital 90 nm CMOS," in *Proceedings of the IEEE International Solid-State Circuits Conference Digest of Technical Papers (ISSCC'04)*, pp. 264–265, February 2004.

[8] Y. Shimizu, S. Murayama, K. Kudoh, H. Yatsuda, and A. Ogawa, "A 30 mW 12b 40MS/s subranging ADC with a high-gain offset-canceling positive-feedback amplifier in 90nm digital CMOS," in *IEEE International Solid-State Circuits Conference Digest of Technical Papers (ISSCC'06)*, pp. 802–811, San Francisco, Calif, USA, February 2006.

[9] A. Matsuzawa, "Design challenges of analog-to-digital converters in nanoscale CMOS," *IEICE Transactions on Electronics*, vol. E90-C, no. 4, pp. 779–785, 2007.

[10] H. Masuda, T. Kida, and S. I. Ohkawa, "Comprehensive matching characterization of analog CMOS circuits," *IEICE Transactions on Fundamentals of Electronics, Communications and Computer Sciences*, vol. E92-A, no. 4, pp. 966–975, 2009.

[11] R. Banchuin, "Process induced random variation models of nanoscale MOS performance: efficient tool for the nanoscale regime analog/mixed signal CMOS statistical/variability aware

design," in *Proceedings of the International Conference on Information and Electronic Engineering*, pp. 6–12, Bangkok, Thailand, 2011.

[12] R. Banchuin, "Complete circuit level random variation models of nanoscale MOS performance," *International Journal of Information and Electronics Engineering*, vol. 1, no. 1, pp. 9–15, 2011.

[13] K. Hasegawa, M. Aoki, T. Yamawaki, and S. Tanaka, "Modeling transistor variation using α-power formula and its application to sensitivity analysis on harmonic distortion in differential amplifier," *Analog Integrated Circuits and Signal Processing*, vol. 72, no. 3, pp. 605–613, 2012.

[14] A. R. Brown and A. Asenov, "Capacitance fluctuations in bulk MOSFETs due to random discrete dopants," *Journal of Computational Electronics*, vol. 7, no. 3, pp. 115–118, 2008.

[15] Y. Li and C. H. Hwang, "High-frequency characteristic fluctuations of nano-MOSFET circuit induced by random dopants," *IEEE Transactions on Microwave Theory and Techniques*, vol. 56, no. 12, pp. 2726–2733, 2008.

[16] M. H. Han, Y. Li, and C. H. Hwang, "The impact of high-frequency characteristics induced by intrinsic parameter fluctuations in nano-MOSFET device and circuit," *Microelectronics Reliability*, vol. 50, no. 5, pp. 657–661, 2010.

[17] H. S. Kim, C. Chung, J. Lim, K. Park, H. Oh, and H. K. Kang, "Characterization and modeling of RF-performance (fT) fluctuation in MOSFETs," *IEEE Electron Device Letters*, vol. 30, no. 8, pp. 855–857, 2009.

[18] R. Banchuin, "The probabilistic model of random variation in nanoscale MOSFET's high frequency performance," in *Proceedings of the 6th WSEAS International Conference on Computer Engineering and Applications, and Proceedings of the 2012 American Conference on Applied Mathematics*, pp. 240–245, January 2012.

[19] M. J. M. Pelgrom, A. C. J. Duinmaijer, and A. P. G. Welbers, "Matching properties of MOS transistors," *IEEE Journal of Solid-State Circuits*, vol. 24, no. 5, pp. 1433–1440, 1989.

[20] K. Kuhn, "Variability in nanoscale CMOS technology," *Science China Information Sciences*, vol. 54, no. 5, pp. 936–945, 2011.

[21] L. L. Lewyn, T. Ytterdal, C. Wulff, and K. Martin, "Analog circuit design in nanoscale CMOS technologies," *Proceedings of the IEEE*, vol. 97, no. 10, pp. 1687–1714, 2009.

[22] H. Abebe, H. Morris, E. Cumberbatch, and V. Tyree, "Compact gate capacitance model with polysilicon depletion effect for MOS device," *Journal of Semiconductor Technology and Science*, vol. 7, no. 3, pp. 131–135, 2007.

[23] R. T. Howe and C. G. Sodini, *Microelectronics: An Integrated Approach*, Prentice Hall, Upper Saddle River, NJ, USA, 1996.

[24] G. Cijan, T. Tuma, and A. Burmen, "Modeling and simulation of MOS transistor mismatch," in *Proceedings of the 6th Eurosim*, pp. 1–8, Ljubljana, Slovenia, 2007.

[25] T. Altiok and B. Melamed, *Simulation Modeling and Analysis with ARENA*, Academic Press, New York, NY, USA, 2007.

[26] S. A. Klugman, H. H. Panjer, and G. E. Willmot, *Loss Models: From Data to Decisions*, John Wiley & Sons, London, UK, 2008.

[27] Predictive Technology Model, http://ptm.asu.edu.

[28] A. H. Haddad, *Probabilistic Systems and Random Signals*, Prentice Hall, Upper Saddle River, NJ, USA, 2006.

[29] W. W. Hines, D. C. Montgomery, D. M. Goldsman, and C. M. Borror, *Probability and Statistics in Engineering*, John Wiley & Sons, London, UK, 2003.

[30] M. Conti, P. Grippa, S. Orcioni, and C. Turchetti, "Parametric yield formulation of MOS IC's affected by mismatch effect," *IEEE Transactions on Computer-Aided Design of Integrated Circuits and Systems*, vol. 18, no. 5, pp. 582–596, 1999.

[31] A. Cathignol, S. Mennillo, S. Bordez, L. Vendrame, and G. Ghibaudo, "Spacing impact on MOSFET mismatch," in *Proceedings of the IEEE Conference on Microelectronic Test Structures (ICMTS'08)*, pp. 90–95, Edinburgh, UK, March 2008.

[32] C. M. Mezzomo, A. Bajolet, A. Cathignol, R. Di Frenza, and G. Ghibaudo, "Characterization and modeling of transistor variability in advanced CMOS technologies," *IEEE Transactions on Electron Devices*, vol. 58, no. 8, pp. 2235–2248, 2011.

Journal of
Engineering

The Scientific
World Journal
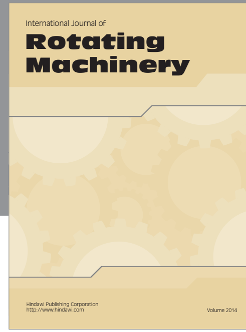
International Journal of
Rotating
Machinery
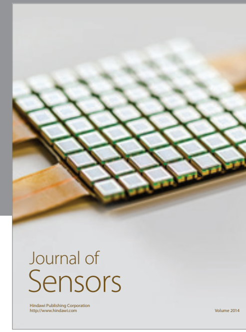
Journal of
Sensors
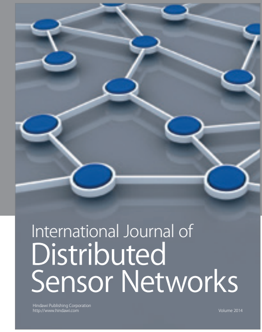
International Journal of
Distributed
Sensor Networks
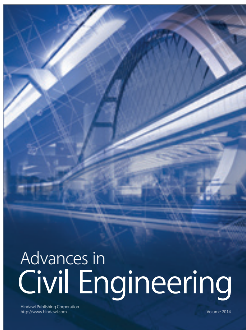
Advances in
Civil Engineering

Hindawi
Submit your manuscripts at
http://www.hindawi.com
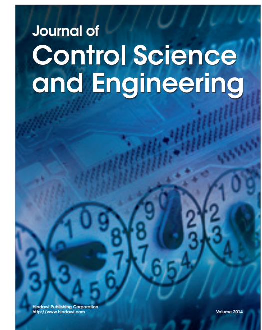
Journal of
Control Science
and Engineering

Journal of
Robotics

Journal of
Electrical and Computer
Engineering
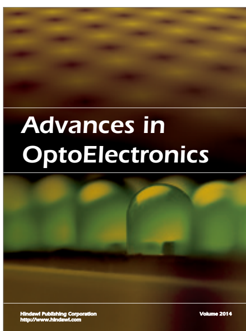
Advances in
OptoElectronics

VLSI Design

International Journal of
Navigation and
Observation
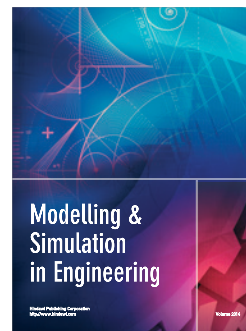
Modelling &
Simulation
in Engineering

International Journal of
Aerospace
Engineering

International Journal of
Chemical Engineering
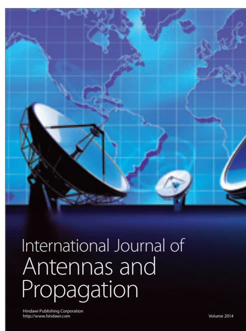
International Journal of
Antennas and
Propagation
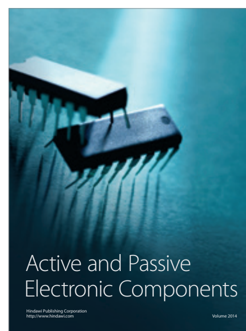
Active and Passive
Electronic Components
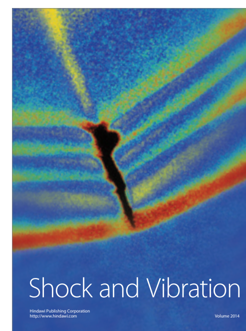
Shock and Vibration
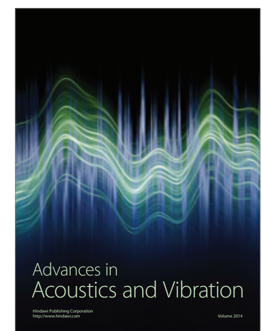
Advances in
Acoustics and Vibration